Russian Geology and Geophysics
Vol. 44, No. 9, pp. 855-866, 2003

Geologiya i Geofizika
UDC 548.4 + 552.333.5

Ni-RICH SULFIDE INCLUSIONS IN EARLY LAMPROITE MINERALS

V.V. Sharygin, L.N. Pospelova, S.Z. Smirnov, and N.V. Vladykin*

United Institute of Geology, Geophysics and Mineralogy, Siberian Branch of the RAS, 3 prosp. Akad. Koptyuga, Novosibirsk, 630090, Russia
** Institute of Geochemistry, Siberian Branch of the RAS, 1a ul. Favorskogo, Irkutsk, 664033, Russia*

Magmatic sulfide inclusions were found in early lamproite minerals from three localities: in olivine-1 of olivine hyalolamproite from Smoky Butte (Montana, USA), in olivine-1 of olivine orendite from Leucite Hills (Wyoming, USA), in orthopyroxene and phlogopite of fortunite from SE Spain. Sulfide blebs usually coexist with fluid and silicate melt inclusions in the host mineral. Occasionally they are found in silicate melt inclusions. Sulfide inclusions contain the following assemblages: pentlandite + chalcopyrite, monosulfide solid solution (Mss) + chalcopyrite, violarite — in the Smoky Butte lamproites; Mss + pentlandite and Mss + chalcopyrite in the Leucite Hills orendites; pentlandite + heazlewoodite, pentlandite + pyrrhotite and pentlandite + godlevskite — in the SE Spain fortunites. Pentlandite broadly varies in Ni/(Ni+Fe) ratio from 0.44 to 0.71. The Smoky Butte Mss has the highest concentrations of Ni (up to 58.2 wt.%) and is close to ideal (Ni,Fe)S (Me/S — 0.98–1.00), while the Leucite Hills Mss contains up to 27.5 wt.% Ni and has a composition intermediate between hexagonal $(Fe,Ni)_9S_{10}$ (Me/S — 0.9) and monoclinic $(Fe,Ni)_7S_8$ (Me/S — 0.875) compositions. Chalcopyrite is similar to ideal composition of the $CuFeS_2$-type. Pyrrhotite compositions vary from FeS to $(Fe,Ni)_9S_{10}$. Ni-rich minerals were found in enstatite of fortunites. They are identified chemically as heazlewoodite solid solution (Ni — 51.1–62.4, Fe — 8.5–17.6, S — 28.7–30.9 wt.%) and godlevskite and/or godlevskite solid solution (Ni — 57.3–62.9, Fe — 4.4–10.3, S — 32.1–32.6 wt.%). Probable composition for initial sulfide melt (ISM) calculated for globules vary for different lamproite localities. In the Smoky Butte lamproites it is undersaturated in sulfur and close in composition to pentlandite (Me/S — 1.10) with approximately equal Ni/(Ni+Fe) ratio (0.51–0.53) and contains up to 33.3 wt.% Ni and up to 5.3 wt.% Cu. Initial sulfide melt in fortunites is also depleted in sulfur (Me/S — 1.11–1.21), but it shows broad variations in Ni content, from 27 to 51 wt.%. Initial sulfide melt in the Leucite Hills orendites is saturated in sulfur (Me/S — 0.91) and contains up to 23.4 wt.% Ni and up to 5.1 wt.% Cu.

The presence of sulfide globules indicates that a small volume of sulfide melt was separated from the silicate liquid at the early stage of evolution of a primitive lamproite magma under $T \gg 1000$ °C, $P \gg 1$ kbar and $f_{O_2} \ll$ NNO. High Ni concentrations in the initial mantle substratum from which a primitive lamproite magma is derived is likely to be responsible for the Ni-rich composition of the initial sulfide melt.

Lamproite, liquid immiscibility, sulfide globule, monosulfide solid solution, chalcopyrite, pentlandite, heazlewoodite, godlevskite, violarite

INTRODUCTION

Recently, sulfide inclusions have been minutely studied in the minerals of alkaline basalts, kamafugites, and kimberlites, as well as in the minerals of mantle xenoliths, megacrysts, and xenocrysts (e.g., diamond). It was established that Fe–Ni–Cu-sulfide blebs are constantly present in these minerals and indicate that sulfide melt is of great importance in magma generation and petrogenesis in mantle and crustal conditions [1–15]. However, in

Table 1

Phase and Chemical Composition of Sulfide Inclusions in Lamproite Minerals

Phase composition of inclusions	Phase	*n*	Fe	Ni	Co	Cu	S	Total	Fe	Ni	Co	Cu	S	Me/S	Ni/(Ni+Fe)	Ni/Fe
			wt.%						at.%							
In olivine-1 of olivine hyalolamproite, Smoky Butte (Montana, USA)																
Pn + Cp	Pn	2	28.79	37.37	0.17	0.46	33.30	100.09	23.42	28.92	0.13	0.33	47.19	1.12	0.55	1.23
Pn + Cp	Pn	2	28.43	37.57	0.17	0.68	33.19	100.04	23.16	29.12	0.13	0.49	47.10	1.12	0.56	1.26
Mss + Cp	Mss	1	4.36	56.32	0.00	3.42	35.49	99.59	3.55	43.64	0.00	2.45	50.36	0.99	0.92	12.29
Pn + Cp	Pn	2	26.55	39.70	0.10	0.09	33.43	99.87	21.63	30.77	0.08	0.06	47.45	1.11	0.59	1.42
Pn + Cp	Pn	1	26.76	39.75	0.20	0.10	33.13	99.94	21.83	30.85	0.15	0.07	47.09	1.12	0.59	1.41
Viol	Viol	2	1.07	45.47	0.13	1.60	41.50	99.77	8.64	33.75	0.10	1.10	56.41	0.77	0.80	3.91
Mss + Cp	Mss	2	3.20	58.27	0.00	2.69	35.81	99.97	2.59	44.93	0.00	1.92	50.56	0.98	0.95	17.32
Mss + Cp	MSS	2	5.52	53.03	0.00	5.51	35.79	99.85	4.48	40.96	0.00	3.93	50.62	0.98	0.90	9.14
Mss + Cp	Mss	2	5.93	55.03	0.00	3.68	35.46	100.10	4.81	42.46	0.00	2.62	50.11	1.00	0.90	8.83
Mss + Cp	Cp	1	30.37	0.14	0.00	34.28	34.91	99.70	25.01	0.11	0.00	24.81	50.07	1.00	0.00	0.00
Pn + Cp	Pn	2	29.11	37.35	0.17	0.17	33.31	100.11	23.67	28.89	0.13	0.12	47.18	1.12	0.55	1.22
	Cp	1	30.50	0.21	0.00	34.30	34.92	99.93	25.07	0.16	0.00	24.77	49.99	1.00	0.01	0.01
	ISM		29.32	31.78	0.14	5.29	33.55	100.08	23.88	24.62	0.11	3.79	47.60	1.10	0.51	1.03
Pn + Cp	Pn	2	27.30	39.21	0.11	0.19	33.18	99.99	22.26	30.41	0.08	0.14	47.12	1.12	0.58	1.37
	Cp	1	30.67	0.21	0.00	34.19	34.90	99.97	25.20	0.16	0.00	24.69	49.95	1.00	0.01	0.01
	ISM		27.81	33.36	0.09	5.29	33.44	99.99	22.69	25.90	0.07	3.79	47.54	1.10	0.53	1.14
In olivine-1 of olivine orendite, Leucite Hills (Wyoming, USA)																
Mss + Pn	Mss	6	34.73	25.59	0.61	0.00	38.72	99.65	27.33	19.15	0.45	0.00	53.07	0.88	0.41	0.70
	Mss + Pn	1	33.43	27.40	0.56	0.04	38.61	100.04	26.26	20.47	0.42	0.03	52.83	0.89	0.44	0.78
Mss + Cp	Mss	1	33.34	27.40	0.47	0.15	38.69	100.05	26.17	20.46	0.35	0.10	52.91	0.89	0.44	0.78
	Cp	1	31.24	0.64	0.07	32.91	34.91	99.77	25.68	0.50	0.05	23.78	49.99	1.00	0.02	0.02
	ISM		33.03	23.39	0.41	5.06	38.12	100.01	26.10	17.58	0.31	3.52	52.49	0.91	0.40	0.67
Mss + Cp	Mss + Cp	1	33.18	19.93	0.37	8.04	38.32	99.84	26.27	15.01	0.28	5.59	52.85	0.89	0.36	0.57
In enstantite of fortunite (SE Spain)																
Pn + Cp	Pn ± Cp	1	28.36	30.99	0.09	7.25	33.23	99.92	23.21	24.13	0.07	5.21	47.38	1.11	0.51	1.04
Pn + Gd*	Pn	1	18.43	48.15	0.06	0.11	33.20	99.95	15.08	37.48	0.05	0.08	47.32	1.11	0.71	2.49
	Gd	1	10.33	57.29	0.00	0.22	32.12	99.96	8.54	45.05	0.00	0.16	46.25	1.16	0.84	5.28
	ISM		16.00	50.89	0.04	0.14	32.88	99.95	13.13	39.73	0.03	0.10	47.00	1.13	0.75	3.03
Pn + Gd*	Gd	1	4.44	62.85	0.00	0.05	32.62	99.96	3.67	49.37	0.00	0.04	46.93	1.13	0.93	13.47
Pn + Hzss	Pn	2	25.76	40.72	0.27	0.06	33.20	100.01	21.01	31.58	0.21	0.04	47.16	1.12	0.60	1.50
	Hzss	2	8.54	62.36	0.00	0.26	28.65	99.81	7.24	50.27	0.00	0.19	42.30	1.36	0.87	6.95
	ISM		18.87	49.38	0.16	0.14	31.38	99.93	15.63	38.89	0.13	0.10	45.26	1.21	0.71	2.49

Table 1 **(continued)**

Phase composition of inclusions	Phase	*n*	Fe	Ni	Co	Cu	S	Total	Fe	Ni	Co	Cu	S	Me/S	Ni/(Ni+Fe)	Ni/Fe
			wt.%						at.%							
Pn	Pn	1	27.28	38.91	0.23	0.06	33.40	99.88	22.23	30.15	0.18	0.04	47.40	1.11	0.58	1.36
Pn	Pn	1	25.18	40.52	0.12	0.50	33.51	99.83	20.53	31.43	0.09	0.36	47.59	1.10	0.60	1.53
Pn + Hzss	Pn	4	28.59	37.96	0.07	0.02	33.28	99.92	23.29	29.42	0.05	0.01	47.23	1.12	0.56	1.26
	Hzss	1	12.51	57.37	0.07	0.09	29.77	99.81	10.51	45.83	0.06	0.07	43.55	1.30	0.81	4.36
Pn + Po	Pn	2	36.40	29.76	0.35	0.04	33.35	99.90	29.55	22.98	0.27	0.03	47.17	1.12	0.44	0.78
	Po	1	62.22	1.11	0.00	0.02	36.56	99.91	49.00	0.83	0.00	0.01	50.15	0.99	0.02	0.02
	ISM		38.98	26.90	0.32	0.04	33.67	99.90	31.55	20.71	0.24	0.03	47.47	1.11	0.40	0.66
Pn + Po	Po	1	60.91	0.28	0.00	0.01	38.78	99.98	47.31	0.21	0.00	0.01	52.47	0.91	0.00	0.00
Hzss	Hzss	1	17.56	51.15	0.08	0.25	30.90	99.94	14.59	40.43	0.06	0.18	44.73	1.24	0.73	2.77
Pn + Hzss	Pn + Hzss	1	20.23	45.84	0.16	0.14	33.46	99.83	16.53	35.63	0.12	0.10	47.62	1.10	0.68	2.16
Pn + Hzss	Pn	1	29.78	36.64	0.25	0.02	33.25	99.95	24.25	28.38	0.19	0.02	47.16	1.12	0.54	1.17
Po + Pn	Po	1	57.62	3.97	0.00	0.28	37.92	99.79	45.12	2.96	0.00	0.19	51.73	0.93	0.06	0.07
Pn + Fe-ox	Pn	2	28.14	38.17	0.20	0.01	33.35	99.87	22.93	29.58	0.15	0.01	47.33	1.11	0.56	1.29

Note. Pn — pentlandite $(Fe_xNi_{11-x})_{9\pm y}S_9$; Cp — chalcopyrite $CuFeS_2$; Mss — monosulfide solid solutions $(Fe_xNi_{1-x})_{1-y}S$; Viol — violarite $(Fe_xNi_{1-x})Ni_2S_4$; Gd — godlevskite $(Fe_xNi_{1-x})_9S_8$ or godlevskite solid solution $(Fe_xNi_{1-x})_{7\pm y}S_6$; Hzss — heazlewoodite solid solution $(Fe_xNi_{1-x})_{3\pm y}S_2$; Po — pyrrhotite $Fe_{1-x}S$; Fe-ox — cubic iron oxide (wüstite or magnetite); ISM — calculated sulfide melt; *n* — number of analyses.

*** Sulfide blebs in melt inclusions (Pn + Gd or Pn + Hzss).**

the world literature there are few publications concerning the presence of sulfides in lamproites [16–23]. Pentlandite and pyrrhotite have been found to coexist with talc in pseudomophs after olivine and with other sulfides (chalcopyrite, pyrite, sphalerite, and galena) in the groundmass of olivine-phlogopite lamproites of the Argyle pipe (Western Australia) [16]; pyrite and pyrrhotite, in the groundmass of hyalolamproites from Smoky Butte (Montana, USA); chalcopyrite, in the matrix of olivine lamproites of the Ellendale-11 pipe (Western Australia), and galena, in the groundmass of jumillites from SE Spain [20–23]. Rounded grains of djerfisherite were identified in the groundmass of leucite lamproite from Napoleon Bay (Buffin Island, Canada) [18]. However, taking into account that the above-mentioned rocks underwent different degrees of secondary alterations, the genesis of these sulfides cannot be regarded unambiguously as primary, since they could form at the postmagmatic stage as well. Only chalcopyrite found earlier as a crystalline phase of melt inclusions in leucite of wyomingites from Leucite Hills (Wyoming, USA) and olivine-leucite hyalolamproites from Oskar Plug (Western Australia) is of clearly magmatic origin [17].

We have revised the most well-known varieties of lamproites (Western Australia, USA, SE Spain) with the purpose to detect magmatic sulfide inclusions in early minerals. Such inclusions have been found only in early minerals of three varieties of lamproites: in olivine-1 of olivine hyalolamproites from Smoky Butte (USA), in orthopyroxene and phlogopite of fortunites from SE Spain, and olivine-1 of olivine orendites from Leucite Hills (USA). Preliminary data on these sulfides were published in [20–23]. This paper is the study of the chemical and phase composition of early sulfide inclusions and *PT*-conditions of their entrapment.

The composition of sulfide minerals was determined using a "Camebax-Micro" probe at 20 kV and 50–60 nA, with beam size of 1–2 μm. Pyrrhotite, chalcopyrite, nickeline, and Fe-Ni-Co alloy were used as standards. The inaccuracy of measurements for major elements was less than 2–3%. To study composition, we used sulfide blebs

Table 2

Chemical Composition (wt.%) of Early Minerals of Lamproites Containing Sulfide Inclusions

Occurrence	Rock	Mineral	*n*	SiO_2	TiO_2	Cr_2O_3	Al_2O_3	FeO	MnO	MgO	CaO	NiO	BaO	Na_2O	K_2O	F	Total	Mg#	Fe_2SiO_4*	Ni_2SiO_4*
Leucite Hills	Olivine orendite	Olivine	2	41.17	0.00	0.00		7.86	0.11	50.75	0.01	0.10					99.99	92.00	7.98	0.10
Smoky Butte	Olivine-phlogopite hyalolamproite	Olivine-1	c	40.78	0.04	0.07		9.20	0.15	48.93	0.13	0.74					100.04	90.46	9.44	0.73
			r	40.60	0.06	0.04		10.68	0.16	48.00	0.16	0.38					100.09	88.90	11.02	0.38
			c	40.66	0.05	0.04		10.14	0.17	48.29	0.17	0.59					100.11	89.46	10.44	0.58
			r	40.50	0.06	0.01		10.93	0.18	47.74	0.16	0.45					100.02	88.61	11.29	0.44
			c	40.91	0.07	0.06		8.64	0.14	49.35	0.14	0.71					100.01	91.05	8.85	0.69
			r	40.45	0.04	0.06		11.17	0.21	47.42	0.16	0.44					99.96	88.32	11.57	0.44
			c	41.02	0.03	0.05		8.04	0.10	49.94	0.10	0.71					99.99	91.71	8.21	0.70
			r	40.55	0.07	0.07		10.68	0.14	47.87	0.15	0.53					100.06	88.87	11.03	0.53
			c	41.01	0.03	0.08		7.84	0.10	50.00	0.10	0.76					99.92	91.91	8.01	0.75
			r	40.52	0.07	0.06		11.20	0.15	47.61	0.16	0.37					100.14	88.34	11.58	0.37
Fortuna	Fortunite	Orthopyroxene	c	58.55	0.10	0.24	0.11	3.69	0.06	36.56	0.40	0.32					100.03	94.64	5.29	0.44
			r	57.83	0.14	0.24	0.22	5.62	0.09	35.07	0.56	0.14					99.91	91.75	8.14	0.19
			c	58.25	0.11	0.31	0.14	4.34	0.07	36.07	0.48	0.18					99.95	93.67	6.25	0.25
			r	57.10	0.16	0.20	0.34	8.07	0.13	33.13	0.71	0.13					99.97	87.97	11.82	0.18
		Phlogopite	c	39.54	3.14	0.53	12.70	4.83	0.01	23.11	0.00		0.12	0.34	9.95	3.21	97.47	89.50		
			r	38.45	5.84	0.56	12.79	8.48	0.02	18.09	0.02		0.38	0.41	9.45	3.62	98.10	79.17		

Note. Mg# = 100Mg/(Mg + Fe); *n* — number of analyses; c — core, and r — rim of grain.

*** For orthopyroxene the concentrations of $Fe_2Si_2O_6$ and $Ni_2Si_2O_6$ are given.**

of more than 10 μm in size (Table 1). Sulfide phases were identified from chemical compositions and optical properties. Pentlandite, monosulfide solid solution (Mss), heazlewoodite, pyrrhotite, chalcopyrite, violarite, and godlevskite were found in sulfide blebs from lamproites of various types. We have also determined the composition of early minerals of lamproites containing sulfide blebs (Table 2).

SULFIDE INCLUSIONS IN EARLY MINERALS

Olivine hyalolamproites, Smoky Butte (Montana, USA). Sulfide inclusions were found in hypidiomorphic, sometimes resorbed grains of olivine-1 (2–5 mm in size, Mg# = Mg/(Mg + Fe) — 0.87, 0.5–0.8 wt.% NiO). Normally they occur as solitary minute blebs (5–12 μm) mainly in the marginal zones of olivine-1 (Fig. 1, *a*, *b*). Larger globules (30–35 μm) are rare. Occasionally sulfide blebs within one inclusions coexist with melt inclusions, less often, with Cr-spinel crystals (54–56 wt.% Cr_2O_3, 21.7–30 wt.% FeO_{tot}, 1.7–2.9 wt.% Al_2O_3, 4.6–5.7 wt.% TiO_2, and 0.1–0.5 wt.% NiO) [21, 24]. The magmatic inclusions in olivine-1 demonstrate a remarkable zoning: sulfide blebs occur closer to the center of crystal than melt inclusions do. Sulfide globules consist of the following mineral assemblages: pentlandite + chalcopyrite, Mss + chalcopyrite, and violarite. Chalcopyrite in large amounts (to 10–15% of the total volume) is present only in large inclusions, whereas in small blebs it forms a thin outer rim 1–2 μm (see Fig. 1, *b*, *d*). It is noteworthy that in the largest and most resorbed grains of olivine-1 some of the sulfide blebs making contacts with groundmass glass are partly replaced by hydroxides and contain only relics of sulfides.

Olivine orendite, North Table Mountain, Leucite Hills (Wyoming, USA). Rare accumulations of sulfide globules have been found in large (>5 mm) rounded olivine grains (Mg# — 0.92, 0.1 wt.% NiO) partly resorbed and surrounded by phlogopite. This olivine is, probably, xenogenous for orendites [25]. Minute blebs (0.5–6 μm) form trails in the host mineral, while large inclusions (to 110 μm) were found only at the intersections of these trails (Fig. 1, *e*). Sulfide inclusions usually coexist with fluid and less often, melt inclusions. Occasionally olivine contains solitary Cr-spinel crystals (60–80 μm). The arrangement of sulfide inclusions implies that they are secondary for host olivine. Sulfide globules consist of the following assemblages: Mss + pentlandite or Mss + chalcopyrite, pentlandide forming very thin (<1 μm) oriented segregations in Mss (see Fig. 1, *f*), and chalcopyrite is confined to the margins of globules.

Fortunite, Fortuna (SE Spain). Sulfides occur as solitary blebs (5–20 μm) in orthopyroxene phenocrysts (Mg# — 0.88–0.95, 0.13–0.32 wt.% NiO), less seldom, in phlogopite phenocrysts (Mg# — 0.8–0.9). Sometimes they form sulfide globules (up to 3–10 μm) in melt inclusions in enstatite and, occasionally, sulfide-melt inclusions (Fig. 2, *a*). Normally sulfide blebs coexist with melt and fluid inclusions, in places, decorating growth zones in orthopyroxene (see Fig. 2, *a*, *b*, *e*). In rare cases together with secondary (pseudosecondary?) fluid inclusions they form chains in the marginal zones of enstatite. Sulfide blebs in orthopyroxene consist of the following assemblages: pentlandite + heazlewoodite, less often, pentlandite + pyrrhotite, and pentlandite + chalcopyrite (see Fig. 2, *d*, *f*). Monomineral inclusions of pentlandite and heazlewoodite are also common. Large inclusions (>20) may contain iron-oxide octahedral phase (magnetite or wüstite, <6 μm in size, see Fig. 2, *c*). Sulfide globules in melt inclusions consist of pentlandite and godlevskite or pentlandite and heazlewoodite. In pentlandite-heazlewoodite assemblages, the latter typically make up the central zone, whereas pentlandite forms rims around it (Fig. 2, *e*, *f*).

CHEMICAL COMPOSITION OF SULFIDES

According to microprobe analysis, nickel phases (pentlandite, heazlewoodite, Ni-rich Mss, godlevskite, and violarite) are predominant in sulfide blebs from early minerals of lamproites, whereas pyrrhotite and chalcopyrite are present in minor amounts (Table 1).

Pentlandite is the most abundant mineral among nickel sulfides in blebs from lamproites of Smoky Butte and Fortuna. This mineral from Smoky Butte is characterized by a minor predominance of Ni over Fe (Ni/Ni + Fe) = 0.55–0.59 and is rather close to ideal $Ni_{4.5}Fe_{4.5}S_8$, whereas pentlandite from blebs in fortunites (Fig. 3) has wider variations in these minerals (Ni/(Ni + Fe) = 0.44–0.71), very high Ni contents (up to 48 wt./%) in some pentlandites being related to the entrapment of heazlewoodite phase (see Table 1).

Monosulfide solid solution (Mss) is typical of blebs in lamproites from Smoky Butte and Leucite Hills, but its compositions from various occurrences differ strongly. Mss in hyalolamproites from Smoky Butte have the highest contents of Ni (53.0–58.3 wt.%) and high Ni/(Ni + Fe) = 0.90–0.92 and are close to ideal (Ni,Fe)S (Me/S = 0.98–1.00, see Fig. 3). The content of Cu in them also varies (2.7–5.5 wt.%), which seems to be due to the entrapment of the smallest segregations of chalcopyrite (Table 1). It is probable that Mss was replaced by millerite as a result of solid-phase reactions at low temperatures (<200 °C). A phase (Mss?) with close contents of Ni and

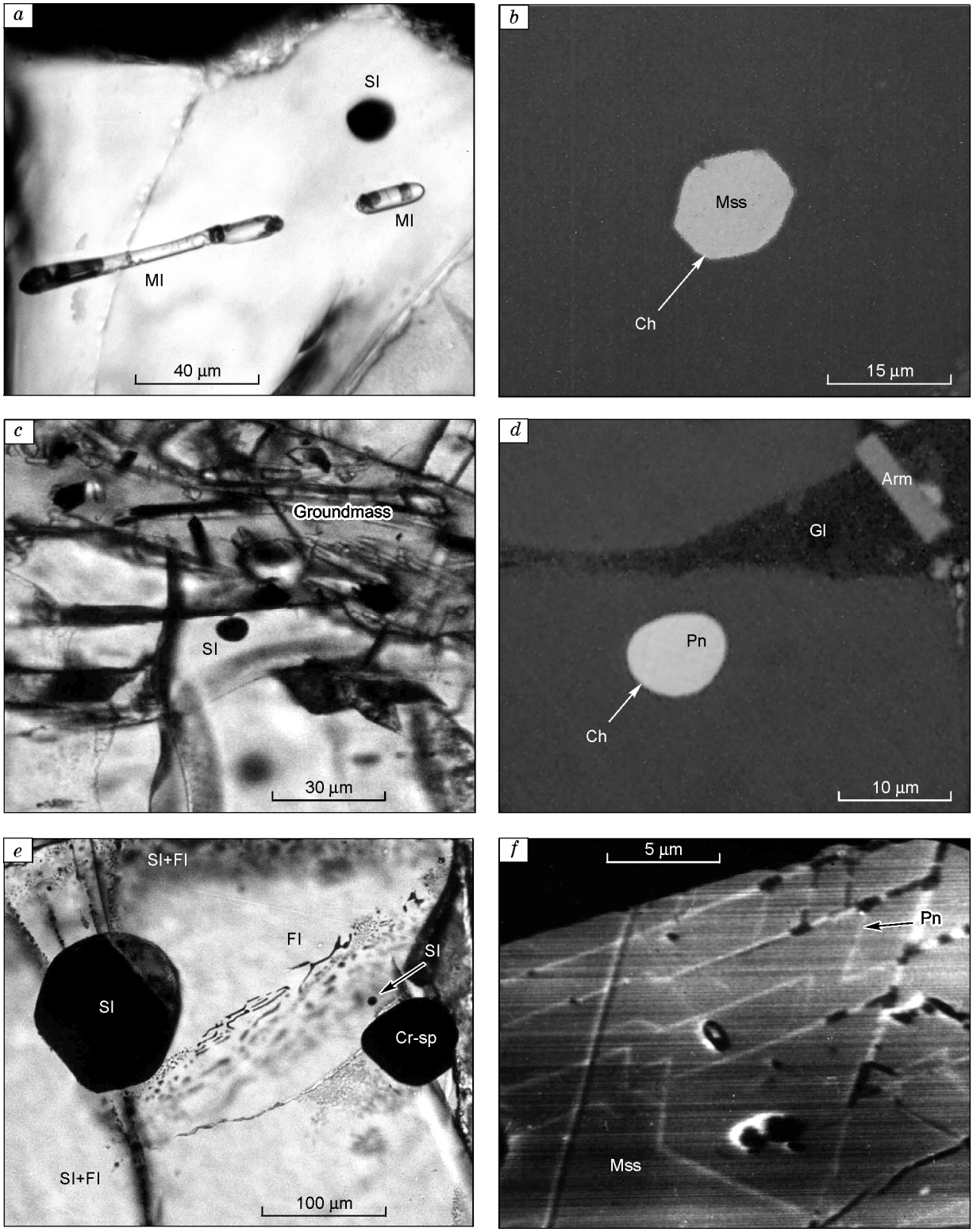

Fig. 1. Sulfide inclusions in early minerals of lamproites from Smoky Butte, Montana, and Leucite Hills, Wyoming. *a* — Coexisting sulfide and melt inclusions in the central zone of olivine-1 from olivine hyalolamproite of Smoky Butte (transmitted light); *b* — sulfide inclusions (see *a*) composed of Mss with a thin rim of chalcopyrite (reflected light); *c*, *d* — sulfide inclusions on the periphery of olivine-1 from the Smoky Butte olivine hyalolamproite: *c* — transmitted light, *d* — phase composition of inclusion — pentlandite with a thin rim of chalcopyrite, reflected light; *e*, *f* — a large sulfide inclusion coexisting with Cr-spinel and secondary sulfide and fluid inclusions in olivine-1 of olivine orendite from Leucite Hills: *e* — transmitted light, *f* — fragment of a large sulfide inclusion with oriented segregations of pentlandite in Mss (scanning microscope, in back electrons). Inclusions: SI — sulfide, MI — melt, FI — fluid; Gl — glass; Arm — armalcolite; Cr-sp — Cr-spinel, Mss — monosulfide solid solution; Pn — pentlandite; Ch — chalcopyrite.

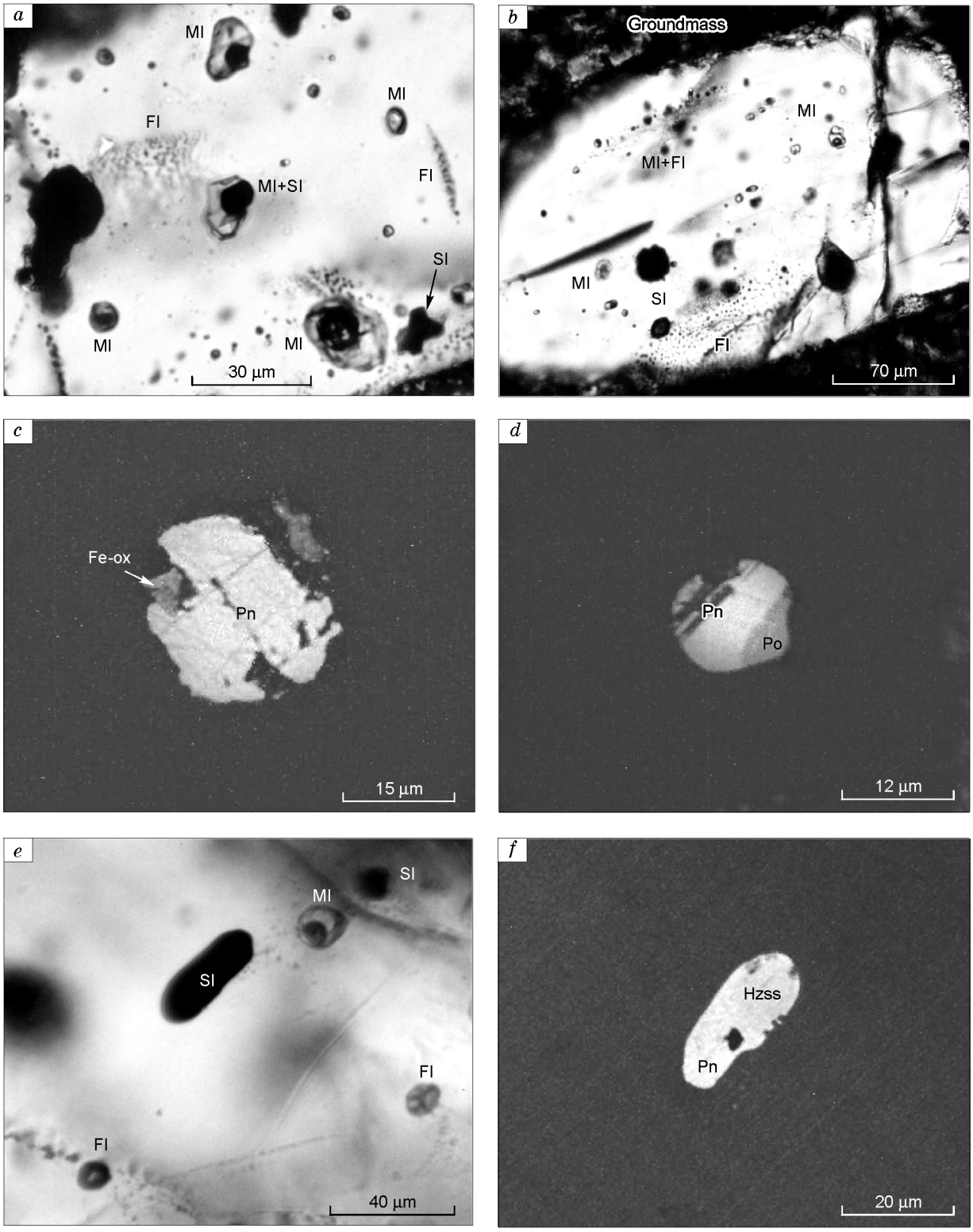

Fig. 2. Sulfide inclusions in orthopyroxene of lamproites from Fortuna, Southeastern Spain. *a* — Coexisting melt, fluid, and sulfide inclusions in orthopyroxene (transmitted light); *b* — distribution of inclusions in an orthopyroxene phenocryst (transmitted light); *c* — sulfide inclusion (see *b*) composed of pentlandite and Fe-oxide phase (reflected light); *d* — two-phase sulfide inclusion (pentlandite + pyrrhotite) in orthopyroxene (reflected light); *e*, *f* — sulfide inclusion coexisting with melt and fluid inclusions: *e* — transmitted light, *f* — phase composition of inclusion — heazlewoodite phase + pentlandite (reflected light). Fe-ox — Fe-oxide phase (wüstite or magnetite); Po — pyrrhotite; Hzss — heazlewoodite solid solution. Other symbols follow Fig. 1.

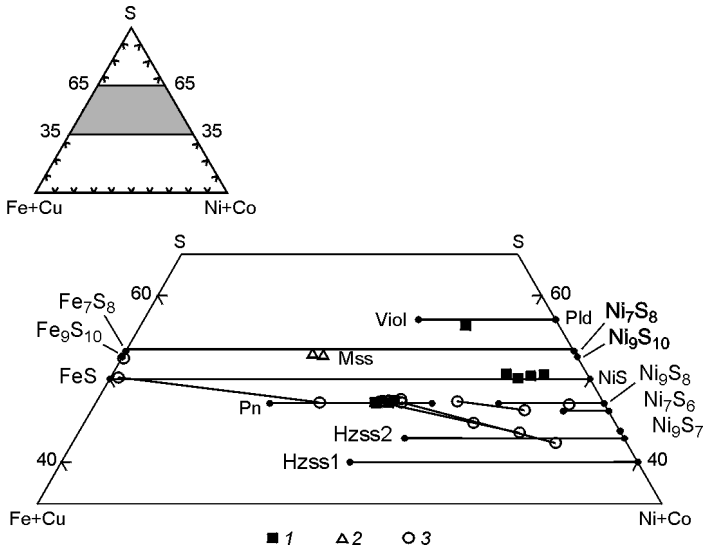

Fig. 3. Composition of Fe-Ni sulfides from early lamproite minerals on the diagram (Fe + Cu)–(Ni + Co)–S. *1* — Smoky Butte (Montana, USA); *2* — Leucite Hills (Wyoming, USA); *3* — Fortuna (SE Spain). The lines connect coexisting phases. Viol — violarite, Pld — polydymite, Hzss1, Hzss2 — heazlewoodite solid solutions on the basis of Ni_3S_2 and Ni_4S_3, respectively; data from [28, 29]. Data for solid solution Ni_9S_8 at 6 GPa and 900 °C are borrowed from [30] and for godlevskite solid solution Ni_7S_6, from [29].

S (53.64 and 37.66 at.%, respectively) was earlier found in association with chalcopyrite and pyrite in olivine megacrysts in basalts from Mount Shasta (California) [4]. Mss from Leucite Hills orendites has lower concentrations of Ni (25.6–.4 wt.%), low Ni/(Ni + Fe) = 0.41, and lacks Cu (0.00–0.15 wt.%, Table 1). By metal/sulfur ratio (0.88–0.89), it has a composition intermediate between hexagonal $(Fe,Ni)_9S_{10}$ (Me/S — 0.9) and monoclinic $(Fe,Ni)_7S_8$ (Me/S — 0.875) pyrrhotites but is closest to $(Fe,Ni)_8S_9$ (Me/S — 0.889, see Fig. 3). Monosulfide solid solutions with close contents of Ni (20–40 wt.%) were earlier found in sulfide inclusions in diamonds, in minerals of some mantle xenoliths, and megacrysts [2, 4, 6, 7, 9, 11, 12, 15].

Chalcopyrite was analyzed in some large globules from lamproites from Smoky Butte and Leucite Hills (Table 1). In general, the compositions of chalcopyrites from these occurrences are close to stoichiometric composition of $CuFeS_2$, being different only in a minor predominance of iron over copper ((Fe + Ni)/Cu = 1.02–1.10 at.%). The concentrations of Ni in chalcopyrites are low (0.2–0.6 wt.%).

Violarite was found only in one monomineral inclusion in olivine-1 in lamproites from Smoky Butte (Table 1). By composition this mineral belongs to thiospinel solid solution violarite $FeNi_2S_4$ — polydymite $NiNi_2S_4$ and contains about 30 mol.% polydymite end-member (Fig. 3). It is noteworthy that violarite or violarite-like phase are common products at phase transformations (T < 450 °C) in sulfide inclusions in diamonds, mantle xenoliths, and megacrysts [4, 6, 7, 10].

In sulfide globules in enstantite of fortunites we analyzed Ni-rich minerals which in chemical composition were identified as heazlewoodite solid solution and godlevskite (or godlevskite solid solution).

Heazlewoodite solid solutions (Hzss) in globules from Fortuna widely vary in composition (51.1–62.4 wt.% Ni, 8.5–17.6 wt.% Fe, and 28.7–30.9 wt.% S, see Table 1), which is, most likely, due to insignificant entrapment of coexisting pentlandite. In general, this phase corresponds to heazlewoodite solid solution Hzss2, distinguished on the basis of Ni_4S_3 [26–28]. One of the compositions is rather close to the heazlewoodite phase $(Ni, Fe)_9S_7$ (Fig. 3) appearing during the exsolution of initial $(Ni,Fe)_9S_8$ formed at 6 GPa and 900 °C in the Fe–Ni–S system [29]. It is worth noting that occasionally the heazlewoodite phase in association with pentlandite is present in sulfide inclusions in diamonds, mantle xenoliths, and megacrysts [6, 9, 12, 15].

Godlevskite (or godlevskite solid solution) was determined only in sulfide globules in melt inclusions. It also strongly varies (57.3–62.9 wt.% Ni, 4.4–10.3 wt.% Fe, and 32.1–32.6 wt.% S, see Table 1 and Fig. 3). One analysis (with high Fe content), most likely, corresponds to phase $(Ni,Fe)_{7\pm x}S_6$ and is, apparently, godlevskite

solid solution, another (with low Fe content) is rather close to godlevskites established in sulfide ores from the Noril'sk group (Russia) and Texmont (Ontario, Canada), in rhodingites from the Bazhenovskoe ultrabasic massif (Central Urals, Russia) [30–33], and phase $(Ni,Fe)_9S_8$ which was found in experimental studies of the phase diagram Fe–Ni–S at 6 GPa and 900 °C [29]. Although the FeS–NiS–Ni_2S_3 part of the Fe–Ni–S system is well studied [26, 27, 29, 34–40], the maximum probable contents of iron in godlevskite-type phases have not been established yet. Up to now, Fe concentration in these phases is assumed to be minimum and their compositions are close to $Ni_{7\pm x}S_6$ and Ni_9S_8. The godlevskite solid solution $Ni_{7\pm x}S_6$ is a high-temperature phase, whereas godlevskite Ni_9S_8 is a low-temperature and stoichiometric phase [26, 28, 38]. However, we do not rule out that we dealt with thin intergrowths of heazlewoodite and pentlandite.

Pyrrhotite was detected in association with pentlandite in enstantite of fortunites. The contents of Ni are no more than 1.5 wt.% (Table 1). As regards Me/S, one of the compositions is close to stoichiometric troilite FeS, whereas the other corresponds to hexapyrrhotite Fe_9S_{10} (see Fig. 3).

Fe-oxide phase was found in association with pentlandite in one of the blebs in enstantite of fortunite. Unfortunately, we managed to perform only a qualitative analysis of this phase because of its small size (< 3 μm). The major component is FeO (>90 wt.%), whereas the concentrations of MgO, Al_2O_3, Cr_2O_3, and MnO are no more than 1 wt.%. By composition, it may correspond either to magnetite or wüstite.

For some polyphase blebs we have calculated the probable composition of initial sulfide melt (see Table 1). The estimations were based on the amount and chemical composition of mineral phases opened on the analyzed surface (error in estimate is 20–30%). The probable composition of sulfide melt for lamproites from Smoky Butte is undersaturated in sulfur, is close to pentlandite (Me/S — 1.10) with nearly equal Ni/(Ni + Fe) = 0.51–0.53, and contains up to 33.3 wt.% Ni and to 5.3 wt.% Cu. Undersaturation in sulfur is also typical of initial sulfide melt in fortunites (Me/S = 1.11–1.21), but its composition strongly varies for different blebs. In two cases it is enriched in Ni and depleted in Fe (Ni/(Ni + Fe) = 0.71–0.75) and in one case (pentlandite + pyrrhotite) iron is predomiannt over nickel (Ni/(Ni + Fe) = 0.40). In contrast to Smoky Butte and Fortuna the initial sulfide melt in orendites from Leucite Hills is saturated with sulfur (Me/S = 0.91), has lower Ni/(Ni + Fe) = 40, and contains 23.4 wt.% Ni and 5.1 wt.% Cu. In general, its composition is very close to the compositions of initial sulfide melt calculated for sulfide inclusions in diamonds, in minerals of some mantle xenoliths, and megacrysts [2, 4, 6, 7, 9, 11, 12, 15].

P-T-f_{O_2} ESTIMATION OF CONDITIONS OF SULFIDE INCLUSION ENTRAPMENT

It is impossible to estimate the conditions of entrapment of sulfide blebs from their phase and chemical composition. The presence of sulfides and absence of coexisting sulfates suggest that oxygen fugacity was considerably lower than NNO buffer [41, 42]. Other parameters of entrapment can be estimated from fluid and melt inclusions which coexist with sulfide blebs.

Thermometric studies of melt inclusions in the early minerals of studied lamproites suggest high temperatures (≫ 1000 °C) at which sulfide melt was trapped [19–21].

According to earlier investigations of lamproites from Smoky Butte [21], olivine crystallized at $T \gg 1250$ °C and $P \geq 2$ kbar. These data suggest that crystallization of olivine-1 and, hence, entrapment of sulfide inclusions occurred ar higher *PT* conditions. Indirect evidence for this is high contents of NiO (to 0.7 wt.%) and low concentrations of CaO (0.10–0.13 wt.%) in the central zones of olivine-1 (see Table 2). Oxygen fugacity calculated from the equilibrium of the olivine–Cr-spinel pair during crystallization of olivine-1 was, probably, 1–2 orders of magnitude higher than the QFM buffer [24].

Homogenization temperature of secondary melt inclusions in olivine-1 of olivine orendite from Leucite Hills is 1010–1100 °C [19, 20]. Unfortunately, cryometric studies of fluid inclusions associated with sulfide blebs did not reveal the presence of high-density carbon dioxide in them. However, most of these inclusions exhibit a halo of minute fluid inclusions, which is, probably, evidence of their decrepitation owing to abrupt pressure release. Low concentrations of CaO (0.01 wt.%) also suggest elevated pressure on crystallization of olivine in orendites from Leucite Hills (see Table 2). The entrapment parameters of sulfide inclusions in orendites from Leucite Hills are, most likely, as follows: >1000 °C, >1 kbar, and $f_{O_2} \approx$ QFM.

Homogenization temperatures of melt inclusions in enstantite of fortunites is 1350 °C [20]. Cryometric studies of melt and fluid inclusions showed that fluid in them has a very low density and, in addition to carbon dioxide, contains other components (triple point from –57.5 to –62.3 °C). The low density of fluid ($\rho = 0.1$ g/cm^3, homogenization into gas phase at 3.2 °C) suggests near-surface crystallization conditions of orthopyroxene in fortunites (0.2–0.3 kbar).

DISCUSSION AND CONCLUSIONS

Thus, the presence of coexisting sulfide, melt, and fluid inclusions in phenocrysts of studied lamproites suggests that at the early stages of evolution the initial lamproitic magma was separated into two components: sulfide and silicate. The number of sulfide blebs evidences that the volume of separated sulfide melt was minor. The entrapment of sulfide inclusions by lamproite minerals took place at temperatures $\gg$ 1100 °C, but pressure could vary.

In spite of probable errors in identification of sulfide phases in blebs and in calculation of initial silicate melt, we can state that the sulfide melt separated from silicate liquid had a Ni-rich composition with a varying sulfur content. It is difficult to say now what physicochemical conditions are responsible for this high Ni concentration in sulfide melt. Lamproites from studied occurrences crystallized from mantle-derived magmas [1–15]. Probable compositions calculated for mantle sulfide melts widely vary but ultranickel (>30 wt.%) compositions are absent. It is worth noting that the majority of early minerals of studied lamproites are enriched in Ni (see Table 2). Thus, the high concentration of Ni in sulfide melt seems to be related to the composition of initial substrate from which a primitive lamproite magma crystallized. It is the Ni-rich composition of the substrate of lamproitic rocks that is, most likely, responsible for the high content of Ni in immiscible sulfide melt.

Solid-phase transformations in sulfide blebs of lamproites hinder correct estimation of their quenching temperature but these data can be obtained from melt inclusions coexisting with sulfides. According to thermometric data on melt inclusions in the early minerals of studied lamproites, melting of glass and quenching of silicate melt took place ar 850–950 °C [20, 21]. It is worth noting once again that we are not sure in the exact identification of some sulfide phases in the blebs from lamproites. These are first of all the phases of heazlewoodite and godlevskite composition in sulfide blebs from Fortuna, since the differences in chemical compositions between high- and low-temperature modifications of these phases are minimal and sometimes cannot be detected by microprobe analysis. Tackling the literature data on the system Fe–Ni–S [26–29, 34–40, 44, 55] reveals controversies as to the presence and behavior of phases of different compositions and variations in their composition in the part FeS–NiS–Ni_3S_2. We will not dwell on details, which are summarized in the work of Kosyakov et al. [28], but we discuss only the high-temperature modifications of heazlewoodite and godlevskite.

The high-temperature heazlewoodite phase (single solid solution on the basis of $Ni_{7\pm x}S_2$ according to one version, or two solid solutions on the basis of Ni_3S_2 (Hzss1) and Ni_4S_3 (Hzss2) according to the other) see revision in [28, 44]) appears at 880 °C by the reaction L + Mss $\rightarrow$ Hzss and disappears when temperature drops to 470 °C by the reaction Hzss $\rightarrow$ Hz (low-temperature stoichiometric heazlewoodite Ni_3S_2) + Pn (pentlandite) and Tn (taenite, γ-(Fe,Ni). Thus, this phase is unstable at room temperatures and under any conditions of quenching inevitably decays into several phases. Most likely, the analyzed Hzss in fortunites from SE Spain is not a homogeneous phase and is submicron solid decay of initial high-temperature Hzss.

The high-temperature godlevskite phase (Gdss, $Ni_{7\pm x}S_6$) appears for the first time in the system Fe–Ni–S at 572 °C by the reaction Hzss2 + Mss $\rightarrow$ Gdss and disappears at 402 °C by the reaction Gdss $\rightarrow$ Gd (low-temperature stoichiometric godlevskite) + Hz. According to data from [28, 38], this phase the same as Hzss is unstable at room temperature. The latest data, however, suggest that Gdss formed during the decay of NiS with a minor deficit of Ni at 450 °C in nitrogen atmosphere can be stable at room temperature [45]. Thus, the existence of two godlevskite phases (Gdss and Gd) in sulfide globules from Fortuna seem not to contradict experimental data in the system Fe–Ni–S.

In conclusion, we emphasize the main results obtained in studies of sulfide blebs in early minerals of lamproites.

1. The presence of sulfide blebs evidences separation of small-volume sulfide melt from silicate liquid at the early stages of evolution of primitive lamproitic magma at $T \gg 1000$ °C, $P \gg 1$ kbar, and $f_{O_2} \ll$ NNO.

2. The initial sulfide melt for lamproites from different regions was Ni-rich, with varying concentrations of sulfur. Obviously, such a composition of sulfide melt is due to the high concentrations of nickel in initial mantle substrate from which a primitive lamproitic magma formed.

3. It is quite probable that the Ni-rich composition of sulfide blebs in early minerals is a specific geochemical feature for lamproites. Only further studies of sulfide inclusions in early minerals from various types of alkaline mantle rocks will confirm or deny this point of view.

We express our sincere thanks to Professor R.H Mitchel (Lakehead University, Thunder Bay, Canada) for providing us lamproites from Smoky Butte. Our thanks also go to Dr. G.R. Kolonin and Dr. E.F. Sinyakova (IMP, SB Division of the RAS, Novosibirsk) for helpful advice and critical remarks.

The work was supported by grant 00-15-98541 from the Russian Foundation for Basic Research.

REFERENCES

1. De Waal, S.A., and L.C. Calk, The sulfides in garnet pyroxenite xenoliths from Salt Lake Crater, Oahu, *J. Petrol.*, **16**, 1, 134–153, 1975.

2. Efimova, E.S., N.V. Sobolev, and L.N. Pospelova, Sulfide inclusions in diamonds and their paragenesis, *Zap. VMO*, part 112, issue 3, 300–310, 1983.

3. Botkunov, A.I., V.K. Garanin, and G.P. Kudryavtseva, Mineral inclusions in garnets from Yakutian kimberlites, *Zap. VMO*, part 112, issue 3, 311–324, 1983.

4. Stone, W.E., M.E. Fleet, and N.D. MacRae, Two-phase nickeliferous monosulfide solid solution (mss) in megacrysts from Mount Shasta, California: a natural laboratory for nickel-copper sulfides, *Amer. Miner.*, **74**, 981–993, 1989.

5. Gurenko, A.A, A.V. Sobolev, and N.N. Kononkova, New data on petrology of ugandites of East-African Rift according to studies of magmatic inclusions in minerals, *Dokl. AN SSSR*, **305**, 6, 1458–1463, 1989.

6. Bulanova, G.P., Z.V. Spetsius, and N.V. Leskova, *Sulfides in diamonds and xenoliths from kimberlite pipes of Yakutia* [in Russian], 119 pp., Nauka, Novosibirsk, 1990.

7. Tal'nikova, S.B., Z.V. Spetsius, and L.A. Pavlova, Phase composition of sulfide inclusions in garnets from kimberlites of Udachnya Pipe, *Miner. Zhurn.*, **12**, 6, 44–51, 1990.

8. Fleet, M.E., and W.E. Stone, Nickeliferous sulfides in xenoliths, olivine megacrysts and basaltic glass, *Contrib. Miner. Petrol.*, **105**, 629–636, 1990.

9. Deines, P., and J.W. Harries, Sulfide inclusion chemistry and carbon isotopes of African diamonds, *Geochim. Cosmochim. Acta*, **59**, 3173–3188, 1995.

10. Szabó, Cs., and R.J. Bodnar, Chemistry and origin of mantle sulfides in spinel peridotite xenoliths from alkaline basaltic lavas, Nógrád-Gömör volcanic field, northern Hungary and southern Slovakia, *Geochim. Cosmochim. Acta*, **59**, 3917–3927, 1995.

11. Barashkov, Yu.P., and S.B. Talnikova, Sulfide inclusions in diamonds and kimberlite minerals: similarities and differences (exemplified by the Udachnaya Kimberlite Pipe, Yakutia), *Geologiya i Geofizika (Russian Geology and Geophysics)*, **37**, 6, 45–55(42–53), 1996.

12. Sobolev, N.V., F.V. Kaminsky, W.L. Griffin, et al., Mineral inclusions in diamonds from the Sputnik kimberlite pipe, Yakutia, *Lithos*, **39**, 135–157, 1997.

13. Shaw, C.S.J., Origin of sulfide blebs in variably metasomatized mantle xenoliths, Quaternary West Eifel volcanic field, Germany, *Can. Miner.*, **35**, 1453–1463, 1997.

14. Stoppa, F., and A. Cundari, Origin and multiple crystallization of the kamafugite-carbonatite association at S.Venanzo-Pian di Celle, Umbria, Italy, *Miner. Magaz.*, **62**, 273–289, 1998.

15. Guo, J., W.L. Griffin, and S. O'Reilly, Geochemistry and origin of sulphide minerals in mantle xenoliths: Qilin, southeastern China, *J. Petrol.*, **40**, 7, 1125–1149, 1999.

16. Jaques, A.L., S.E. Haggerty, H. Lucas, and G.L. Boxer, Mineralogy and petrology of the Argyle (AK1) lamproite pipe, Western Australia, *Geol. Soc. Austr. Spec. Publ.*, **14**, 1, 153–169, 1989.

17. Mitchell, R.H., Coexisting glasses occurring as inclusions in leucite from lamproites: examples of silicate liquid immiscibility in ultrapotassic magmas, *Miner. Magaz.*, **55**, 197–202, 1991.

18. Hogarth, D.D., Mineralogy of leucite-bearing dykes from Napoleon Bay, Baffin Island: multistage Proterozoic lamproites, *Can. Miner.*, **35**, 53–78, 1997.

19. Sharygin, V.V., Evolution of lamproites suggested by melt inclusions in minerals, *Geologiya i Geofizika (Russian Geology and Geophysics)*, **38**, 1, 136–147(142–153), 1997.

20. Sharygin, V.V., *Physicochemical features of crystallization of lamproites according to study of melt inclusions in minerals*, PhD Thesis as a Report [in Russian], 48 pp., OIGGM SO RAN, Novosibirsk, 1997.

21. Sharygin, V.V., L.I. Panina, and N.V. Vladykin, Silicate-melt inclusions in minerals of lamproites from Smoky Butte (Montana, USA), *Geologiya i Geofizika (Russian Geology and Geophysics)*, **39**, 1, 38–54(35–51), 1998.

22. Sharygin. V.V., and L.N. Pospelova, Sulfide inclusions in early lamproite minerals, in *7th IKC, Cape Town: Extended Abstracts*, 794–796, 1998.

23. Sharygin, V.V., Ni-rich sulfide inclusions in early lamproite minerals, *Terra Nostra*, 6 (Abstracts of XV ECROFI, Potsdam, Germany), 265–267, 1999.

24. Sharygin, V.V., Melt inclusions and chromite in lamproites from Smoky Butte, Montana, *7th IKC, Cape Town: Extended Abstracts*, 785–787, 1998.

25. Kuehner, S.M., A.D. Edgar, and M. Arima, Petrogenesis of the ultrapotassic rocks from the Leucite Hills, Wyoming, *Amer. Miner.*, **66**, 663–677, 1981.

26. Lin, R.Y., D.C. Hu, and Y.A. Chang, Thermodynamics and phase relationships of transition metal-sulfur system: I. Transition metal-sulfur systems. II. The nickel-sulfur system, *Met. Trans.*, **9B**, 4, 531–538, 1978.

27. Stolen, S., F. Gronvold, E.W. Westrum, and G.R. Kolonin, Heat capacity and thermodynamic properties of synthetic heazlewoodite, Ni_3S_2, and of high-temperature phase $Ni_{3\pm x}S_2$, *J. Chem. Thermodynamics*, **23**, 77–93, 1991.

28. V.I. Kosyakov, A.G. Kraeva, Zh.N. Fedorova, and E.F. Sinyakova, Topological analysis of evolution of phase equilibria in the Fe-Ni-S system in the range $X_S < 0.5$ along the temperature axis, *Geologiya i Geofizika (Russian Geology and Geophysics)*, **37**, 12, 7–17(5–15), 1996.

29. Leontievskii, K.V., V.A. Kirkinskii, and Zh.N. Fedorova, Phase relationships between sulfide minerals of iron and nickel at 6 GPa and 900 °C, *Geologiya i Geofizika (Russian Geology and Geophysics)*, **33**, 11, 88–95(72–78), 1992.

30. Kulagov, E.A., T.L. Evstigneeva, and O.E. Yushko-Zakharova, Godlevskite, a new sulfide of iron and nickel, *Geologiya Rudnykh Mestorozhdenii*, **11**, 3, 115–121, 1969.

31. Naldrett, A.J., E. Gasparrini, R. Buchan, and J.E. Muir, Godlevskite (β-Ni_7S_6) from the Texmont mine, Ontario, *Can. Miner.*, **11**, 879–885, 1972.

32. Czamanske, G.K., V.E. Kunilov, M.L. Zientek, et al., A proton-microprobe study of magmatic sulfide ores from the Noril'sk-Talnakh district, Siberia, *Can. Miner.*, **30**, 249–287, 1992.

33. Spiridonov, E.M., N.S. Barsukova, N.N. Kononkova, and I.M. Kulikova, Godlevskite Ni_9S_8 of rodingites of Bazhenovskoe ultrabasic massif, Central Urals, *Dokl. RAN*, **356**, 6, 814–816, 1997.

34. Kullerud, G., The Fe–Ni–S system, *Year Book 1962*, 175—189, Carnegie Inst., Wash., 1963.

35. Karup-Müller, S., and E. Makovicky, The phase system Fe–Ni–S at 900°C, *Neues. Jahrb. Miner. Monatsh.*, iss. 8, 373–384, 1998.

36. Misra, K.C., and M.E. Fleet, The chemical compositions of synthetic and natural pentlandite assemblages, *Econ. Geol.*, **68**, 518–539, 1973.

37. Fedorova, Zh.N., and E.F. Sinyakova, Experimental investigation of physicochemical conditions of pentlandite formation, *Geologiya i Geofizika (Russian Journal of Geology and Geophysics)*, **34**, 2, 84–92(79–87), 1993.

38. Stolen, S., H. Fjellvag, F. Gronvold, and E.F. Westrum, Phase stability and structural properties of $Ni_{7\pm x}S_6$ and Ni_9S_8: heat capacity and thermodynamic properties of Ni_7S_6 at temperatures from 5K to 970K and of Ni_9S_8 from 5K to 673K, *J. Chem. Thermodynamics*, **26**, 9, 987–1000, 1994.

39. Sinyakova, E.F., Zh.N. Fedorova, and V.S. Pavlyuchenko, Physicochemical conditions of platinum phase formation in Fe–Ni–S system, *Geologiya i Geofizika (Russian Geology and Geophysics)*, **37**, 5, 39–49(38–47), 1996.

40. Sugaki, A., and A. Kitakaze, High from of pentlandite and its thermal stability, *Amer. Miner.*, **83**, 1–2, 133–140, 1998.

41. Fincham, C.J., and F.D. Richardson, The behaviour of sulfur in silicate and aluminate melts, *Proc. R. Soc. London*, **A233**, 40–62, 1954.

42. Carroll, M.R., and M.J. Rutherford, Sulfide and sulfate saturation in hydrous silicate melts, *J. Geophys. Res.*, **90**, C601–C612, 1985.

43. Mitchell, R.H., and S.C. Bergman, *Petrology of Lamproites*, 447 pp., Plenum Publication, New York, 1991.

44. Kitakaze, A., and A. Sugaki, Study of the $Ni_{3\pm x}S_2$ phase in the Ni–S system with emphasis on the phases of high-form $Ni_3S_2(\beta_1)$ and $Ni_4S_3(\beta_2)$, *Neues Jahrb. Miner. Monatsh.*, iss. 1, 41–48, 2001.

45. Bishop, D.W., P.S. Thomas, and A.S. Ray, Alpha-beta phase re-transformation kinetics in nickel sulphide, *J. Therm. Analyt. Calorim.*, **56**, iss. 1, 429–435, 1999.

Editorial responsibility: N.V. Sobolev Received 10 October 2001